EFFECTS OF MULTIPLE SCLEROSIS ON LOCOMOTOR PATTERN GENERATION

Aswin Farzana Mohamed Ansar, Isabel Souza Shiratsubaki
Kuan-Jung Chiang, Zachary Haiman
Bioengineering, University of California San Diego

Abstract

The locomotor central pattern generator (CPG) is a biological neural network for locomotion that produces rhythmic patterned outputs without sensory feedback found in the spinal cord of vertebrates[1]. The left-right limb coordination is the locomotor gait in limbed animals, with the coordination between left and right neural activities enabled by the presence of commissural interneurons (CINs) [1]. Each rhythm generator has flexor and extensor centers which are responsible for flexor-extensor skeletal muscle coordination, resulting in the the gait of joint movements in limbs. In diseases such as multiple sclcerosis, demylination resulting from neurodegenearation causes the CPG to exhibit spastic symptoms.

To analyze the effects of multiple sclereosis on the mammalian locomotor CPG for bilateral left-right interactions, two models of the neural circuitry for single limb flexor-extensor reflexes were constructed and connected to form a two-level model of locomotor CPG and left-right commissural interactions [1][2]. To reflect the conditions of multiple sclerosis, the conductance of excitatory neurons was increased to reflect the hyperexcitability caused by the demyelination of neurons [3].

1 Background

1.1 Central Pattern Generators

Central pattern generators (CPG) are complex biological neural networks capable of producing rhythmic patterned outputs without any sensory feedback or decendending input [1]. Typically found in the spinal cords of vertebrates, the rhythmic motor patterns produced by central pattern generators are utlized for locomotion via walking, flying, and swimming, and for subconscious processes such as cardiac rhythm and breathing [4]. Though the characteristics of CPGs are based on their biological function, a neural network is classified as a CPG by two key criteria: the network must consist of two or more processes that interact such that each process sequentially increases and decreases, and the result of this interaction causes the system to repeatedly return to its starting condition [5]. For mammalian locomotion, the CPG network for a single limb consists of two dedicated half centers, one for flexors and one for extensors. Each half center has three layers that coordinate flexor and extensor interactions: a rhythm generator (RG) layer, a pattern formation (PF) layer, and a motorneuron (Mn) layer (Figure 1).

The RG layer is an oscillatory network responsible for creating the rhythmic signals and transmitting them to the PF layer below. The PF network recieves the rhythmic input, reshapes the extensor and flexor signals into patterns for the desired behavior, and transmits the signals to the motorneurons. The motorneurons then transmit the signals to the appropriate extensor and flexor muscles to produce the desired behavior in one limb. The CPG of one limb also extends its effect onto the the other limb, facilitating coordinated left-right behavior between the limbs at the motorneuron level and producing the muscle contractions for locomotion.

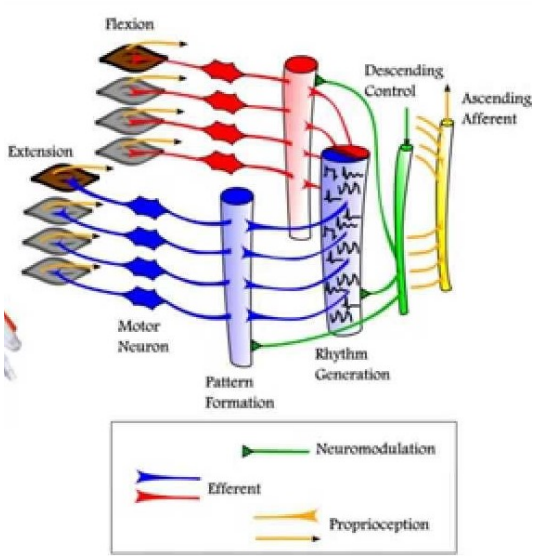

Figure 1: Locomotor CPG general schema. Source: [6].

1.2 Multiple sclerosis

Multiple sclerosis (MS) is an autoimmunte disease in which the immune system attacks the protective myelin sheath of nerve fibers (Figure 2), causing neurodegeneration and communcation problems between the brain and the body [8]. Symptoms of MS can manifest in a variety of ways, dependent on the severity and progression of the disease.In cases of primary progressive multiple sclerosis (PPMS) the disease is characterized by an overall worsening of neurological function represented as an accumulation of disability from the onset of symptoms [9]. One such debilitating symptom that affects over 80 percent of individuals diagnosed with MS is spasticity, defined by the American Association of neurological as a condition in which continous muscles are continuosly contracted. The continuous muscle contractions result from the demyelination of nerve fibers, causing overexciation in nerves and manifesting as flexor and extensor spasms [10].

Therefore, to analyze the effects of multiple sclereosis on the mammalian locomotor CPG for bilateral left-right interactions, two models of the neural circuitry for single limb flexor-extensor reflexes were constructed and connected to form a two-level model of locomotor CPG and left-right commissural interactions [1][2]. To reflect the conditions of MS, the conductance of excitatory neurons was increased to reflect the hyperexcitability caused by the demyelination of neurons [3].

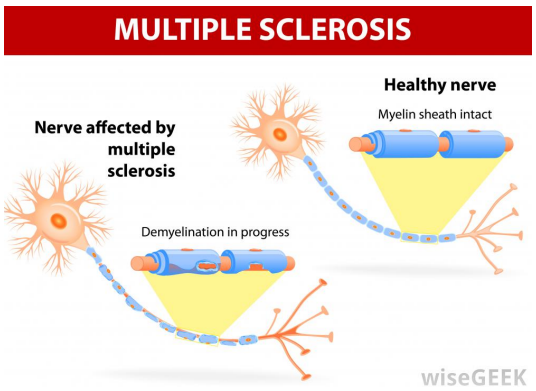

Figure 2: Locomotor CPG general schema. Source: [6].

2 Single Limb Model

The locomotor network is usually modeled by two main different approaches: the population model and the reduced model.

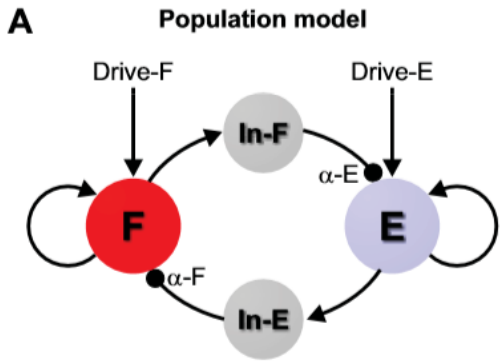

Figure 3: Diagram representing the RG layer in the population model. Source: [11].

2.1 Population Model

In this approach, the Rhythm Generator (RG) layer consists of two population of excitatory neurons (Flexor - F and Extensor - E half centers, Figure 3) and two population of inhibitory interneurons (In-F and In-E, Figure 3). Each population of excitatory neurons represents two hundred neurons, which have intrinsic bursting properties and mutual excitatory synapse. Each inhibitory population represents one hundred neurons, which do not have intrinsic busting properties neither mutual interactions

In this approach, all neurons are modeled in Hodgkin-Huxley Style. The neural membrane potential (V) presents the following equation:

- For E and F half centers:

$$C\frac{dV}{dt} = -I_{Na} - I_{NaP} - I_K - I_L - I_{SynE} - I_{SynI} \tag{1}$$

- For interneurons:

$$C\frac{dV}{dt} = -I_{Na} - I_K - I_L - I_{SynE} - I_{SynI} \tag{2}$$

- For the currents:

$$I_{Na} = g_{Na}.m_{Na}^3.h_{Na}.(V - E_{Na}) \tag{3}$$

$$I_{NaP} = g_{NaP}.m_{NaP}^3.h_{NaP}.(V - E_{Na}) \tag{4}$$

$$I_K = g_K.m_K^4.(V - E_K) \tag{5}$$

$$I_L = g_L.(V - E_L) \tag{6}$$

$$I_{SynE} = g_{SynE}.(V - E_{SynE}) \tag{7}$$

$$I_{SynI} = g_{SynI}.(V - E_{SynI}) \tag{8}$$

$$g_{SynEi}(t) = g_E.(\sum_j wji.\sum_{t_{kj}<t} exp(-\frac{t - t_{kj}}{\tau_{SynE}}) + Drive) \tag{9}$$

$$g_{SynIi}(t) = g_I.(\sum_j wji.\sum_{t_{kj}<t} exp(-\frac{t - t_{kj}}{\tau_{SynI}})) \tag{10}$$

The equations 9 and 10 define the conductance for the excitatory and inhibitory synapses. The weight wji is added in the pre-synaptic event during a spike.

2.2 Reduced Model

In the reduced model, the RG layer consists of two half-centers (Flexor - F and Extensor - E, Figure 4) mutually coupled by inhibitory synapses with conditional bursting properties. Each unit represents a synchronized neural population and each membrane potential represents an average voltage for that population.

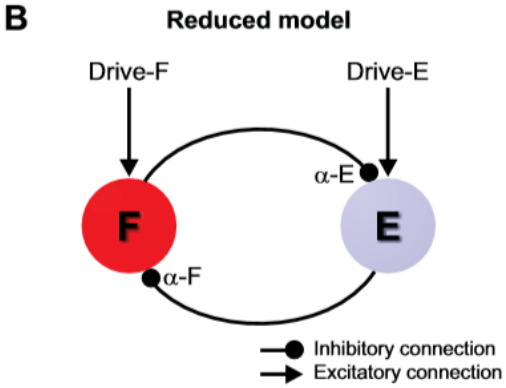

Figure 4: Diagram representing the RG layer in the reduced model. Source: [11].

The equations for this model are given as

$$C\frac{dV}{dt} = -I_{NaP} - I_L - I_{SynE} - I_{SynI} \tag{11}$$

$$I_{NaP} = g_{NaP}.m_{NaP}.h_{NaP}.(V - E_{Na}) \tag{12}$$

$$I_L = g_L.(V - E_L) \tag{13}$$

$$I_{SynE} = g_{SynE}.Drive.(V - E_{SynE}) \tag{14}$$

$$I_{SynI} = g_{SynI}.\alpha.f(V(V_{pre}).(V - E_{SynI}) \tag{15}$$

$$f(V(V_{pre}) = (1 + exp(-\frac{V_{pre} + \theta}{\sigma}))^{-1} \tag{16}$$

Each synaptic output f(V), where f(V) ϵ [0,1], represents the integrated population activity at the corresponding average voltage. The intrinsic RG rhythmogenesis is due to the persistent sodium current I_{NaP} and the slow activity of h_{NaP} activity. In the population model, the interneurons do not contain the NaP dependency. Therefore, they do not create the oscillatory pattern of the CPG.

The considerations for the next layers are described below.

In the PF layer, we have tree neurons mutually coupled by inhibitory synapses. The neuron receiving excitatory synapse from E and F RG-half centers is responsible for facilitating the motorneurone activation and timing the phase transitions without shifting the phases. The equations used to model PF neurons were the same as the equations for E and F RG-half centers.

The last layer consists of the motorneurones. These neurons are located in the muscles. To represent the physiological difference in distribution of Ca ion concentration in the tissue, the membrane potential equation was split into two differential equations (S-Soma; D-Dentrite):

$$C\frac{dV(S)}{dt} = -I_{Na}(S) - I_K(S) - I_{CaN}(S) - I_{K,Ca}(S) - I_L(S) - I_C(S) \tag{17}$$

$$C\frac{dV(D)}{dt} = -I_{NaP}(D) - I_{CaN}(D) - I_{CaL}(D) - I_{K,Ca}(D) - I_L(D) - I_{SynE} - I_{SynI} \tag{18}$$

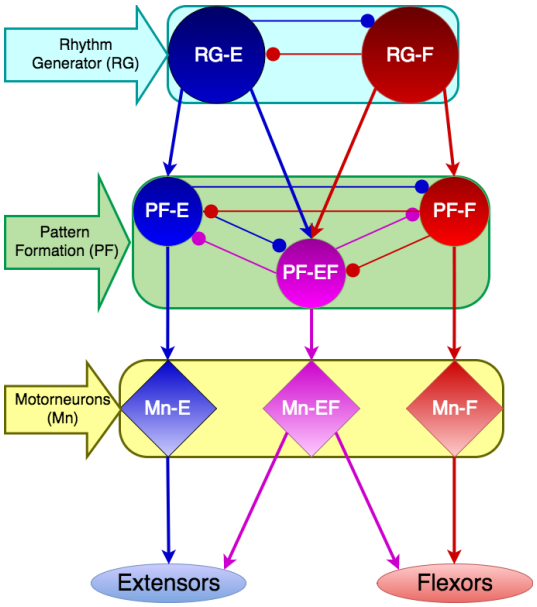

Figure 5: Diagram representing the all the layer in the reduced model for one limb.

The current equations for sodium, potassium and leak current are the same of the previous layers. The other currents are given by:

$$I_{CaN} = g_{CaN}.m_{CaN}^2.h_{CaN}.(V - E_{Ca}) \tag{19}$$

$$I_{CaL} = g_{CaL}.m_{CaL}^2.(V - E_{Ca}) \tag{20}$$

$$I_{k,Ca} = g_{K,Ca}.(V - E_K) \tag{21}$$

The reduced model is used for qualitative analysis of the system dynamics [11], which is suitable for the goals of this project. In addition, this model requires less computation time to be run.

All the parameters used are found in the Appendix.

2.3 Simulation

2.3.1 Single Limb CPG Behavior

The spinal CPG network has half centers for each limb with neuronal population controlling the extensor and flexor of that limb. The simplified single limb CPG network model is shown in Figure 5.

The RG layer consists of neuronal population in a reciprocal inhibitory network between the flexor and extensor centers. The flexor inhibiting the extensor when the flexor is active and firing and vice versa. Thus, this layer facilitates the alternating behavior evident in extensors and flexors during any activity. The drive to the extensor and flexor from the supra-spinal regions contribute to the extensor and flexor dominant rhythm to accomplish voluntary actions. The RG layer is responsible for shuttling the rhythm down to the rest of the network and is noted in the muscle activity.

The PF layer consists three pools of neurons namely the PF- Extensor (PF-E), PF-Flexor (PF-F) and PF-Extensor and Flexor (PF-EF). The PF layer controls the muscle activation providing effective load-bearing and thrust forces. The PF-E and PF-F pools receives the rhythm from the corresponding RG population and the supra-spinal drive. The PF-EF establishes the appropriate balance between the extensor and flexor. Each neuron pool is connected to the other two neuron pools through the reciprocal inhibition to aid with effective balanced motion. The patterns formed are transmitted to the Motor-neuron extensor and flexor pool through the excitatory synapses with its corresponding pattern formation pool and the EF.

The single limb model was tested using two different sets of input drives to observe the extensor and flexor behavior. The first set of drives were used to see the flexor dominant rhythm and the second was to extensor dominant rhythm. The effect of these rhythms on the pattern formation layer and the motor neuron layer were observed. The progression of multiple sclerosis in the spinal CPG neuron pool was observed by varying the excitability.

2.3.2 Rhythm Generation Layer

Although the CPG has an intrinsic oscillatory behavior creating balanced rhythm under normal conditions, voluntary thought can vary the rhythm generated at the CPG based on the activity wanted to be performed. Therefore we observed the extensor and flexor dominant rhythm generated by the RG layer when the supra-spinal drive was not equal. In the first set, we set the flexor drive to be 0.35 and the extensor rhythm to be 0.1. It was observed that the extensor and flexor fired alternately because of the intrinsic reciprocal inhibitory nature creating the oscillation. Also, we were able to observe that the period of flexor neuron pool firing increased depicting the increased activity of the flexor when compared to the extensor. For the Second set, the drives were interchanged, the extensor dominant rhythm was observed in the behavior of the RG neuron pool with a longer extensor activity compared to the flexor.

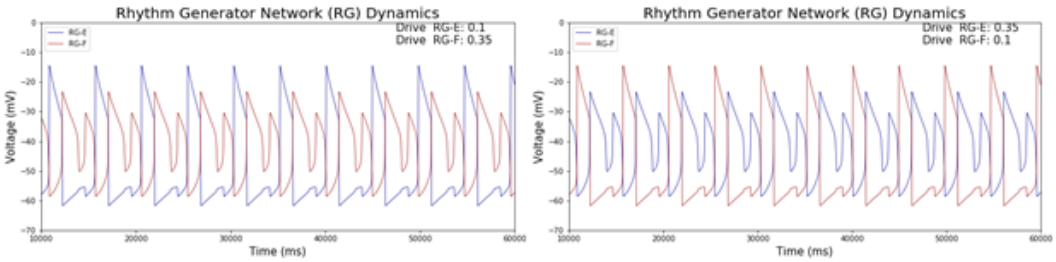

Figure 6: Plots of membrane voltages of the RG layer neuron population showing flexor dominant rhythm and extensor dominant rhythm.

2.3.3 Pattern Formation Layer

We wanted to observe the effects of extensor and flexor dominant rhythm in the neuronal behavior of the PF layer. The reciprocal inhibition between the neuron pools facilitated a controlled periodic pattern generated by the PF layer. The inhibitory effect of the flexor and extensor pattern generation pool over each other and over the PF-EF pool facilitated the controlled extent of activation of each of the centers in the pattern formation. It was observed that the amplitude was reduced depicting the controlled activation based on the drives still carrying the rhythm generated by the rhythm generation layer.

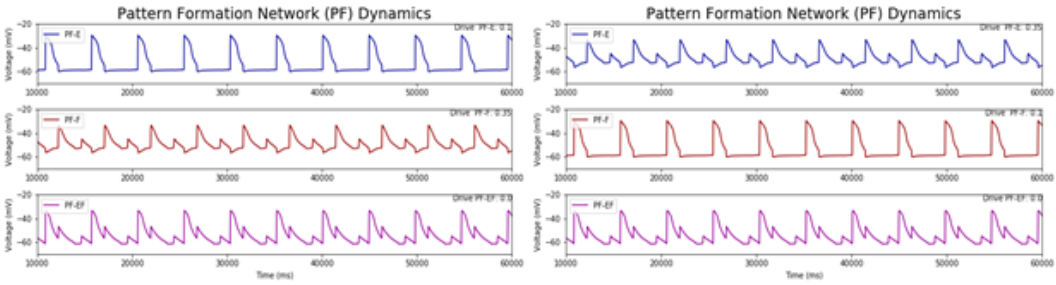

Figure 7: Plots of membrane voltages of the PF layer neuron population showing flexor dominant and extensor dominant patterns.

2.3.4 Motorneuron Layer

We also wanted to observe the effects of the rhythm and the pattern generated at the muscle level observing the behavior of the motor neuron pool. The excitatory synaptic connection between the PF-E and PF-F to the corresponding Extensor and flexor neuron aided in the reflection of the rhythm at the motor neuron level. The motor neuron behavior depicted a balanced extensor and flexor action. The amplitude of the less dominant center was high but the duration of activation was lower when compared to the dominant center. Thus, proving the balanced Extensor flexor action at the muscular level produced by the CPG network to facilitate effective body balancing in any activity intended.

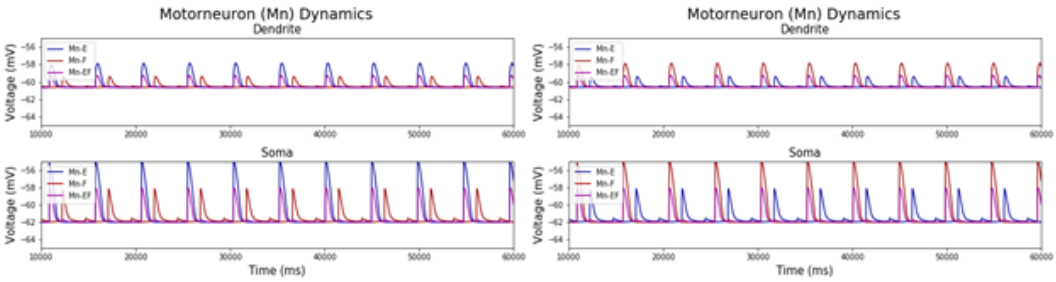

Figure 8: Plots of membrane voltages of the motor neuron layer neuron population showing flexor dominant and extensor dominant dynamics.

2.3.5 Disease

MS is characterized by the hyperexcitability due to the degeneration of the insulating myelin sheath of the neurons. This effect was implemented by increasing the conductibility of the synapse at various disease progression levels. The synaptic conductance was increased around 5- 10 % to observe the changes in behavior of the CPG network under mild sclerotic conditions. The behavior of the RG layer does not change as it still has the intrinsic capability to generate the oscillations the results were vivid in the pattern formation layer and the motor neuron layer as shown in Figure 9. It did not produce spasms as the sclerotic conditions are subtle when they start. As the disease progresses under synaptic conductance further increases and the effect of severe sclerosis was observed under Complete degeneration of the myelin sheath. The pattern formation and the motor neuron layer loses the rhythm shuttled from the rhythm generation layer and it shows a continued contraction of both extensor and flexor at the same time. Thus, proving the spasms created in the sclerosis patients as their leg gets locked and they are unable to move effectively. The effect is shown in Figure 10

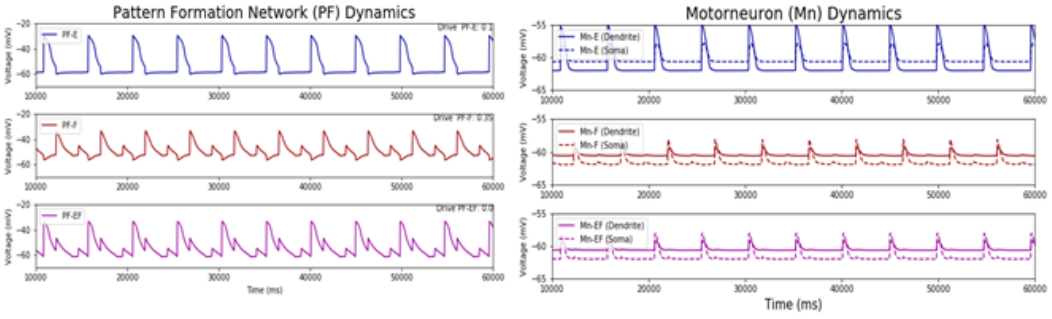

Figure 9: Plots of membrane voltages of the at the mild sclerotic conditions

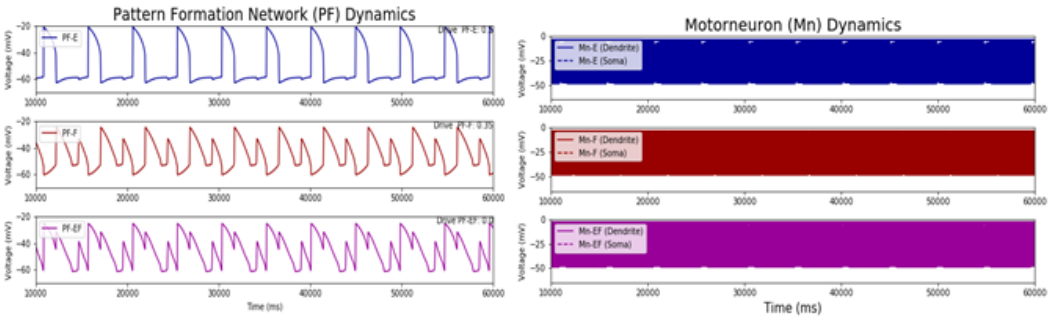

Figure 10: Plots of membrane voltages of the severe sclerotic conditions

3 Left-Right Coordination Model

The logic of left-right coordination is that the rhythm at one part should inhibit the rhythm of the other part. We refer to multiple models from other research and make our own simplified model of left-right coordination as shown in Figure 11. In RG layer, we have inhibitory synapses from flexor at one part to flexor at the other part and excitatory synapses from extensor at one part to flexor at the other part. By these connections, the flexor-dominant rhythm from one part should inhibit the flexor-dominant rhythm at the other part but extensor-dominant rhythm should excite the flexor-dominant one at the other part.

In PF layer, PF neurons are also affected by the RG neurons from the other part. Based on the same logic, inhibitory synapses connects extensor RG neuron from one part to extensor PF neuron at the other part and flexor to flexor as well. Similarly but with a little difference, extensor RG neuron from one side is connected to both the flexor PF neuron and the middle PF neuron with excitatory synapses, and flexor RG neuron is also connected to both extensor PF neuron and the middle one with excitatory synapses.

It is noteworthy that in RG layer, only flexor neurons play the role of post-synapse neurons . This characteristic of the left-right coordination is seen in other research. The reason may be that the flexor is more dominant in the whole CPG. We are not clear about this. However, even if the extensors also play as post-synapse neurons, the basic logic of the left-right coordination remains the same.

To test our model of left-right coordination, we use two different sets of input drive and observe the behavior of our model. The first case is to see whether the rhythm at one part can induce the rhythm in the other part. The second case is to observe the behavior when each part has its own rhythm and whether the stronger rhythm can dominate the rhythm at the other part.

3.1 Case 1: Right Inducing Left

In the first case, we want to see whether rhythm at the right part can induce rhythm at the left part. We set the both input drive of extensor (RG and PF) neurons and flexor (RG and PF) neurons at the left part to zero, so that there should be no rhythm when the left part is not affected by the right part. As for the right part, we set the drive of extensor and flexor neurons to 0.1 and 0.5, so that there should be a flexor dominant rhythm at the right part when there is no left-right coordination.

Figure 12 and 13 show the results of the first simulation. From Figure 12, we can see that there is a flexor dominant rhythm at the right part as expected since the input drive of flexor neuron is larger. However, at the left part, a rhythm is induced even when the input drive at left part is zero. Furthermore, the plot of the membrane voltage of extensor RG neuron at the left part is extremely similar to the flexor at the right part and flexor at the left part is also similar to the extensor at the right part. Then from Figure 13, we can see that PF at the left part have very similar patterns as the right part as well (if the extensor and flexor are reversed).

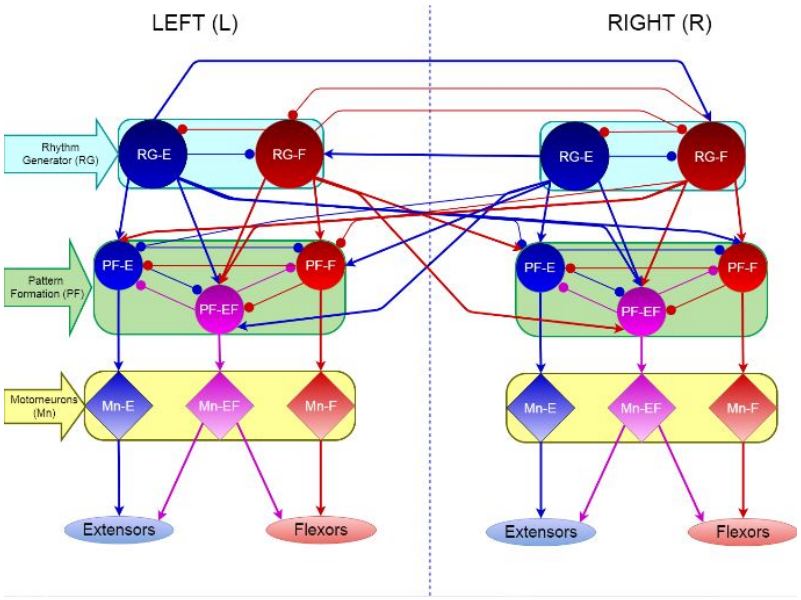

Figure 11: Diagram of the left-right coordination model.

It proves that the flexor-dominant rhythm at the right part can induce a extensor-dominant rhythm at the left part. This makes sense because the logic of left-right coordination in our model is that flexor at one part should be excited by extensor and inhibited by flexor from the other part.

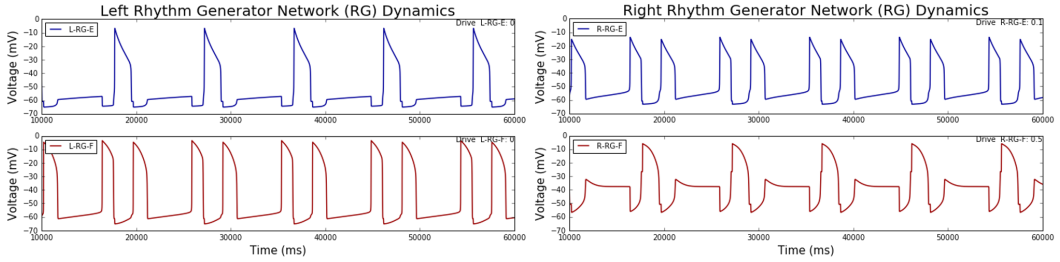

Figure 12: Plots of membrane voltage of RG neurons at left and right part in case 1.

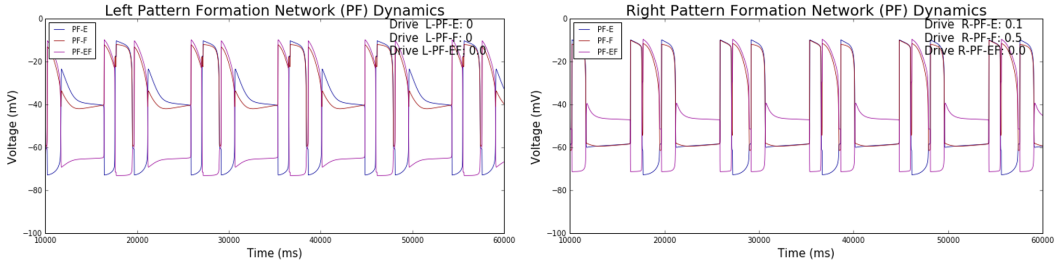

Figure 13: Plots of membrane voltage of PF neurons at left and right part in case 1.

3.2 Case 2: Right Part Reversing Left Part

In the second case, we want to see when both parts have rhythm with different strength, whether the stronger one can dominate and make the rhythm at the other part reverse (extensor dominant to

flexor dominant or vice versa). We set the drive of the extensor and flexor at left part to 0.1 and 0.2, so that the drive should generate slightly flexor-dominant rhythm at left part. As for the right part, we set the drive of the extensor and flexor to 0.05 and 0.55, which leads to a strong flexor-dominant rhythm at the right part.

Figure 14, Figure 15 and Figure 16 show the plots of the membrane voltage at RG layer, PF layer and motor neuron layer. We can see that at the left part, it is hard to tell the rhythm in RG layer is extensor-dominant or flexor-dominant. Extensor has two big spikes while flexor has one big spike and two small spikes in one cycle. However, at the PF layer and especially at the motor neuron layer, it is clear that extensor becomes dominant. Therefore, the result shows that the rhythm at the left part indeed reversed by the right part.

However, the result is not totally as expected. We can see that although the rhythm at the right part is stronger, it is also affected by the left part. In the RG layer, the rhythm is clearly flexor-dominant, but at the PF and motor neuron layer, it is hard to tell whether the rhythm is extensor-dominant or flexor-dominant. This can be discussed in the future work.

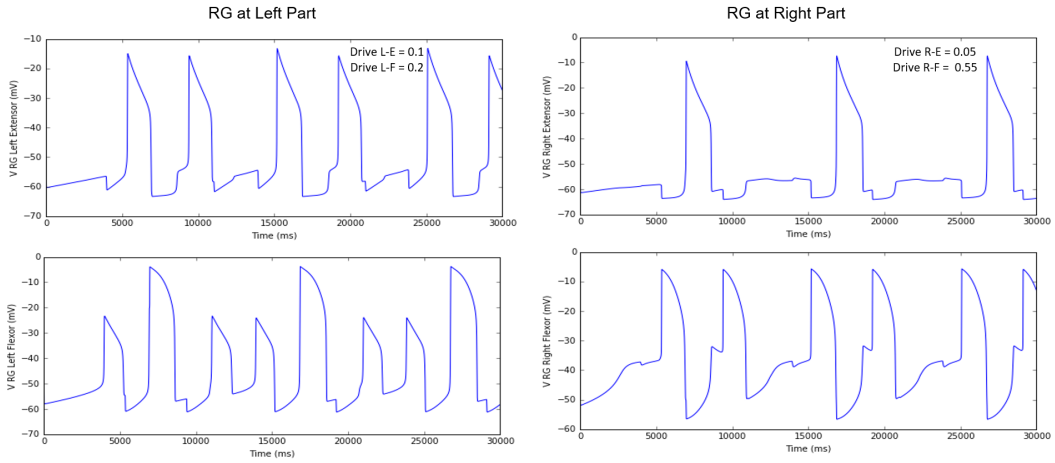

Figure 14: Plots of membrane voltage of RG neurons at left and right part in case 2.

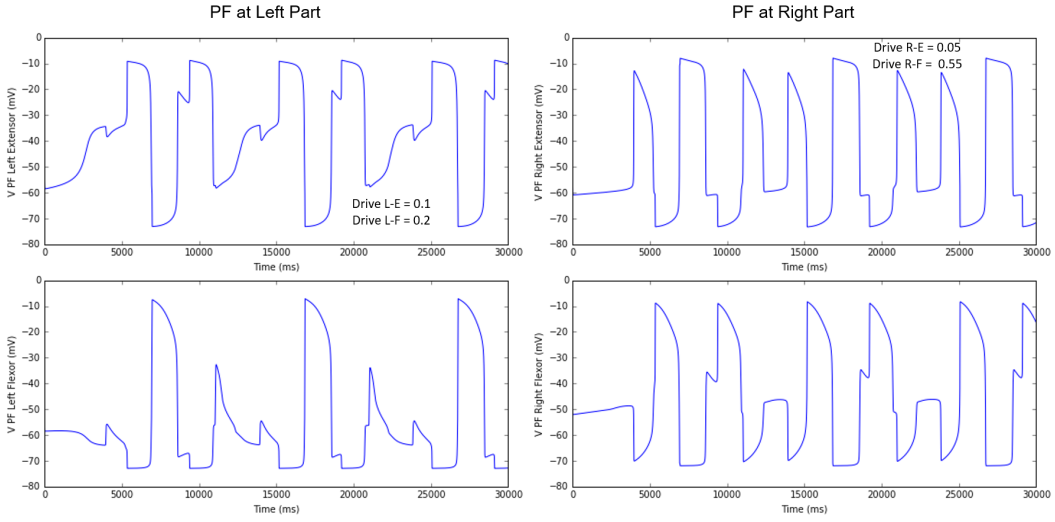

Figure 15: Plots of membrane voltage of PF neurons at left and right part in case 2.

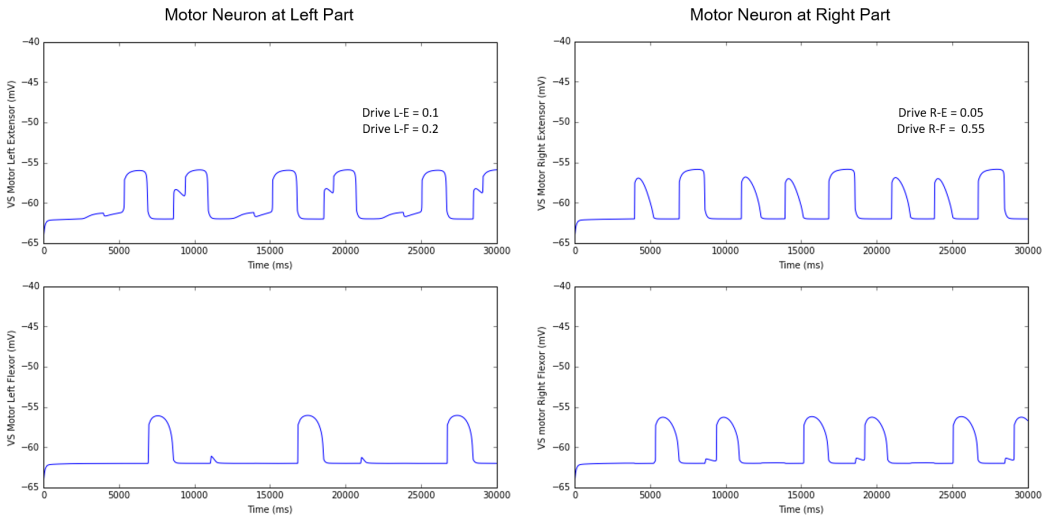

Figure 16: Plots of membrane voltage of motor neurons at left and right part in case 2.

3.3 Disease in Left-Right Coordination Model

Figure 17, Figure 18 and Figure 19 show the effects of Multiple Sclerosis on Left-Right Coordination Model. The adjustment of the parameters is similar to the previous disease discussion in the Single Limb section. We can see that the patterns of both left and right part are still somewhat normal at the RG layer, but at the PF layer, the rhythm patterns become wierd and not clear. At the final layer, the motor neuron layer, the spikes become weird and uneffective ones as same as the ones shown in previous section. The result shows that the left-right coordination model is also affected by the disease.

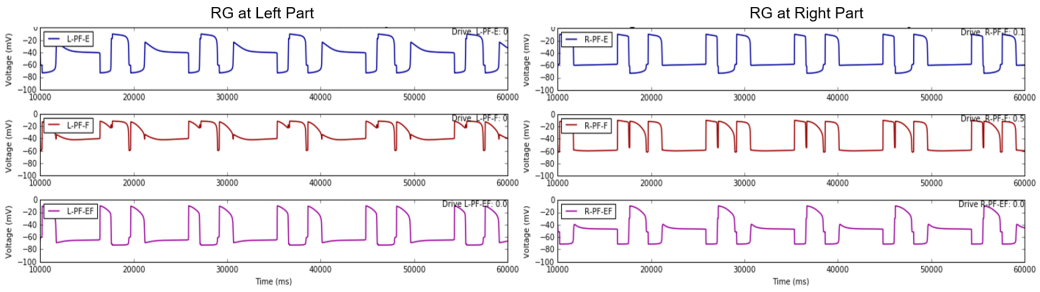

Figure 17: Plots of membrane voltage of RG neurons at left and right part in disease discussion.

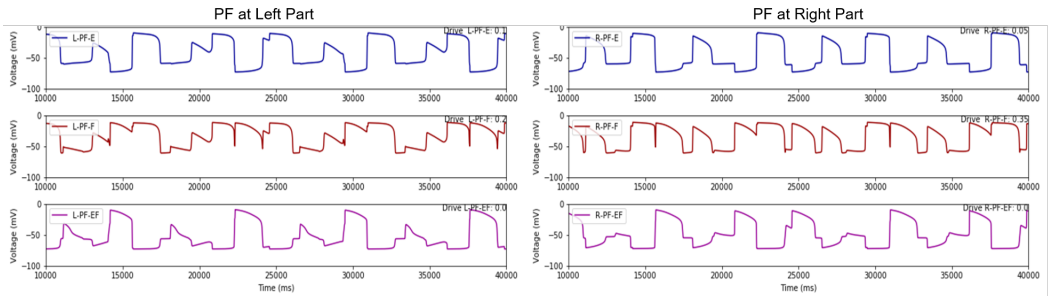

Figure 18: Plots of membrane voltage of PF neurons at left and right part in disease discussion.

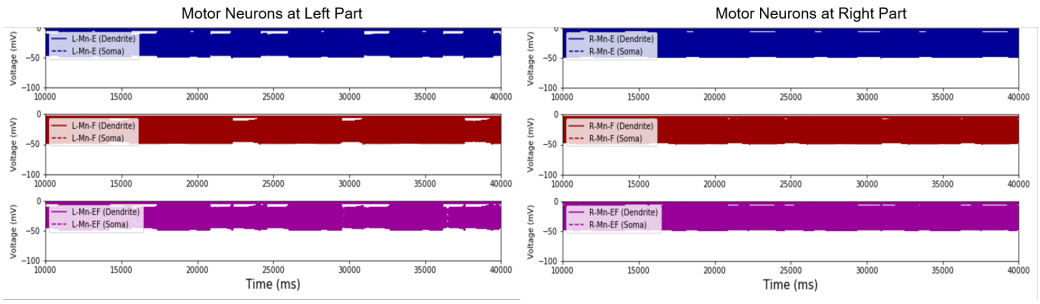

Figure 19: Plots of membrane voltage of motor neurons at left and right part in disease discussion.

4 Future Directions

There are several ways in which the model can be expanded upon in order to further explore left-right coordination and locomotor CPGs in mammalians. For this project, the reduced model was utilized in this experiment to qualitiatively explore the neurodynamics. Therefore, the next steps with the reduced model would be stability analysis on the network to analyze the effects of the supraspinal drive on the network and the critical points for bifurcations. Another direction would include expansion of the reduced model into the physiologoically relevant population network. Through a population model, quantitative information can be gathered and explored for possible therapeutic options to regain locomotion for individuals disabled by the mild to moderate forms of the disease.

Acknowledgments

All implementations and simulations of our models were programmed in Python with BRIAN. All sections of the paper were equally distributed among all four members.

References

[1]. Rybak I, Dougherty K, Shevtsova N. Organization of the Mammalian Locomotor CPG: Review of Computational Model and Circuit Architectures Based on Genetically Identified Spinal Interneurons. eNeuro. 2015;2(5). doi:10.1523/eneuro.0069-15.2015.

[2]. Rybak I, Shevtsova N, Lafreniere-Roula M, McCrea D. Modelling spinal circuitry involved in locomotor pattern generation: insights from deletions during fictive locomotion. The Journal of Physiology. 2006;577(2):617-639. doi:10.1113/jphysiol.2006.118703.

[3]. Demyelination: What Is It and Why Does It Happen?. Healthline. 2017. Available at: https://www.healthline.com/health/multiple-sclerosis/demyelinationsymptoms. Accessed December 15, 2017.

[4]. Marder E, Bucher D. Central pattern generators and the control of rhythmic movements. 2017.

[5]. Bucher D, Haspel G, Golowasch J, Nadim F. Central Pattern Generators. eLS. 2015:1-12. doi:10.1002/9780470015902.a0000032.pub2.

[6]. Nassour J, Hnaff P, Benouezdou F, Cheng G. Multi-layered multi-pattern CPG for adaptive locomotion of humanoid robots. Biological Cybernetics. 2014;108(3):291-303. doi:10.1007/s00422-014-0592-8.

[7]. What Are Motor Neuron Lesions? (with pictures). wiseGEEK. 2017. Available at: http://www.wisegeek.com/what-are-motor-neuron-lesions.htm. Accessed December 16, 2017.

[8]. Multiple sclerosis - Symptoms and causes - Mayo Clinic. Mayoclinicorg. 2017. Available at: https://www.mayoclinic.org/diseases-conditions/multiple-sclerosis/symptoms-causes/syc-20350269. Accessed December 16, 2017.

[9]. Primary progressive MS (PPMS). National Multiple Sclerosis Society. 2017. Available at: https://www.nationalmssociety.org/What-is-MS/Types-of-MS/Primary-progressive-MS. Accessed December 16, 2017.

[10]. AANS — Spasticity. Aansorg. 2017. Available at: http://www.aans.org/Patients/Neurosurgical-Conditions-and-Treatments/Spasticity. Accessed December 16, 2017.

[11]. Ausborn J, Snyder A, Shevtsova N, Rybak I, Rubin J. State-Dependent Rhythmogenesis and Frequency Control in a Half-Center Locomotor CPG. Journal of Neurophysiology. 2017:jn.00550.2017. doi:10.1152/jn.00550.2017.

Appendix

The table below shows the parameters used in the Reduced Model.

Ion channels	
Fast sodium (Na)	$m_{\infty Na} = (1 + \exp(-(V + 34)/7.8))^{-1}$ $\tau_{mNa} = 0\ ms$ $h_{\infty Na} = (1 + \exp((V + 55)/7))^{-1}$ $\tau_{hNa} = 10/(\exp((V + 50)/15) + \exp(-(V + 50)/16))\ ms$ $\bar{g}_{Na} = 500\ nS$
Persistent Sodium (NaP)	$m_{\infty NaP} = (1 + \exp(-(V + 40)/6))^{-1}$ $\tau_{mNaP} = 0\ ms$ $h_{\infty NaP} = (1 + \exp((V + 55)/12))^{-1}$ $\tau_{hNaP} = 4000/\cosh((V + 55)/24)\ ms$ $\bar{g}_{NaP} = 5\ nS$
Potassium rectifier (K)	$m_{\infty K} = (1 + \exp(-(V + 28)/4))^{-1}$ $\tau_{mK} = 3.5/\cosh((V + 40)/40)\ ms$ $\bar{g}_{K} = 40\ nS$
Leak (L)	$g_{L} = 2.8\ nS$
Neuron parameters	
Reversal potentials	$E_{Na} = 50$ mV; $E_{K} = -80$ mV; $E_{SynI} = -75$ mV Population model: $E_{SynE} = -10$ mV; $E_{L} = -65 \pm 0.325$ mV Reduced model: $E_{SynE} = 0$ mV; $E_{L} = -62.5$ mV
Membrane capacitance	$C = 20$ pF
Synaptic/network parameters	
Synaptic parameters	Population model$\bar{g}_{E} = \bar{g}_{I} =$: 0.1 nS; $\tau_{SynE} = \tau_{SynI} = 5$ ms Reduced model: $\bar{g}_{SynE} = \bar{g}_{SynI} = 1$ nS; $\theta = 25$ mV; $\sigma = 5$ mV
Synaptic connections	Population model ($w_{ji} = \bar{w}_{ji} \pm$ SD): F to F: 0.075 ± 0.00375, $p = 0.1$ F to In-F: 0.175 ± 0.00875, $p = 1$ E to E: 0.075 ± 0.00375, $p = 0.1$ E to In-E: 0.175 ± 0.00875, $p = 1$ In-F to E: 0.05 ± 0.005, $p = 1$ ($\Rightarrow \alpha\text{-E} = 5$) In-E to F: 0.05 ± 0.005, $p = 1$ ($\Rightarrow \alpha\text{-F} = 5$) Reduced model: $\alpha\text{-F} = \alpha\text{-E} = 1$

* Parameter values are identical for the two models unless otherwise indicated.

Figure 20: Table for parameters used in the reduced model. Source: [11].